

CHAPTER 4

Characterization Studies

CHAPTER –4

CHARACTERIZATION STUDIES

4.1 X-ray diffraction studies:

X-ray diffraction patterns of powder glass samples were taken using X-ray diffractometer Philips PM 8203 with PW 1390 channel control and PW 1373 goniometer. All the glasses of series 1,2 and 3 were examined for their amorphousness. The diffraction patterns were taken from 0° to 70° with Cu α target. The diffraction spectra showed only big halos not any crystallization peak. X-ray diffraction patterns of few glass samples shown in Figure 4.11, 4.12 and 4.13 for series 1, 2 and 3 respectively, confirmed that the glasses prepared by the quenching technique do not show any crystalline or diffraction peaks, which confirm the amorphous nature of all the prepared glasses in Series 1,2 and 3.

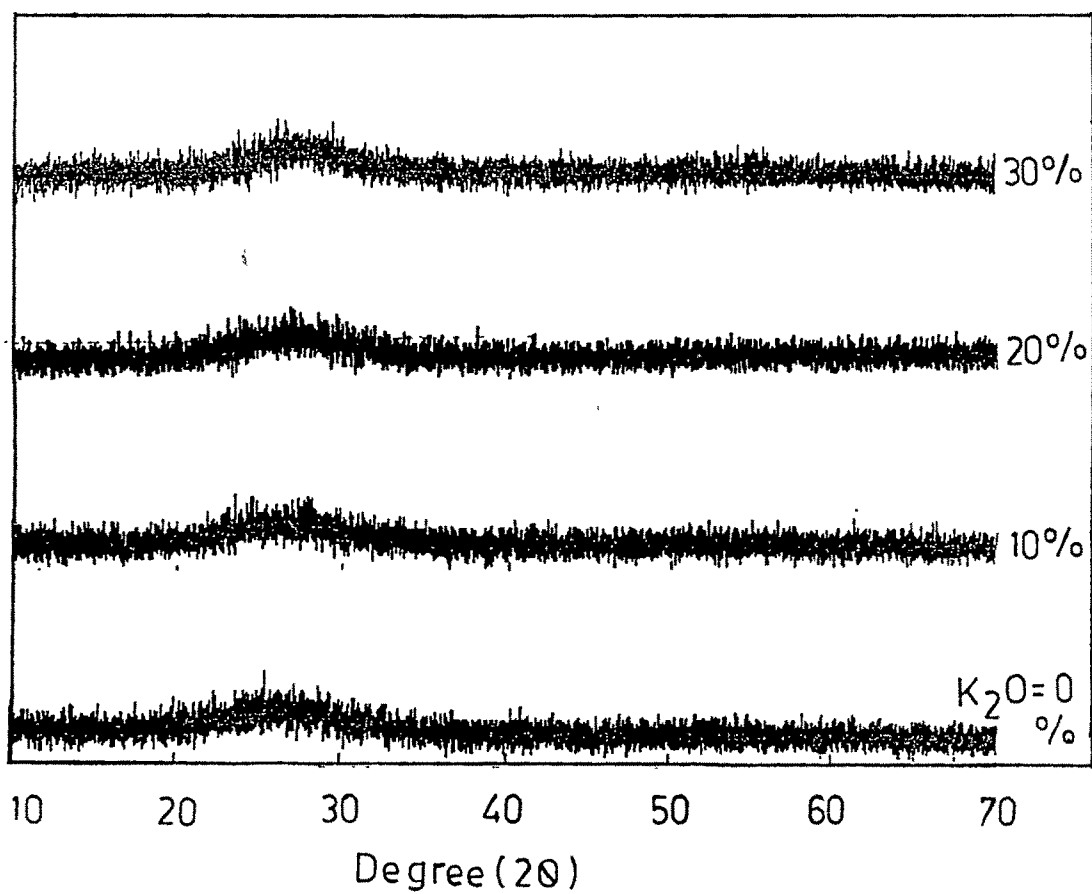


Figure 4.11 : X-ray diffraction pattern of few glass samples of Series 1.

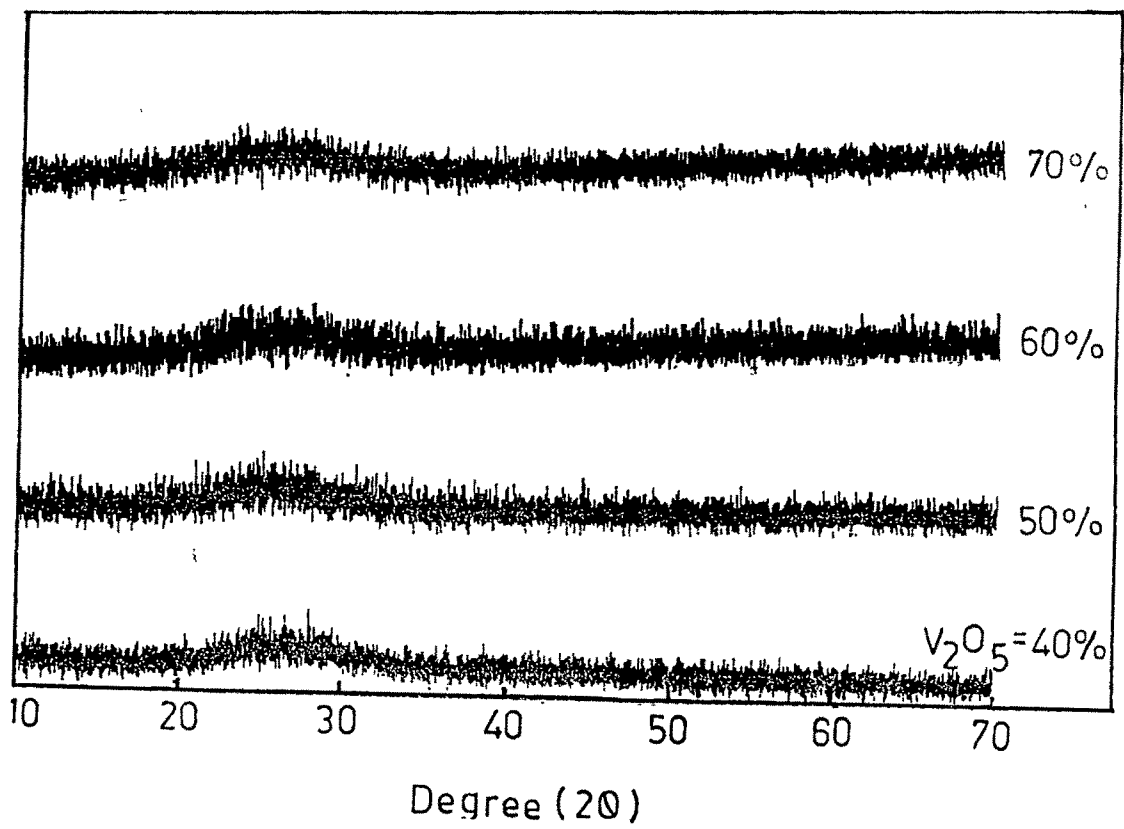


Figure 4.12 : X-ray diffraction pattern of few glass samples of Series 2.

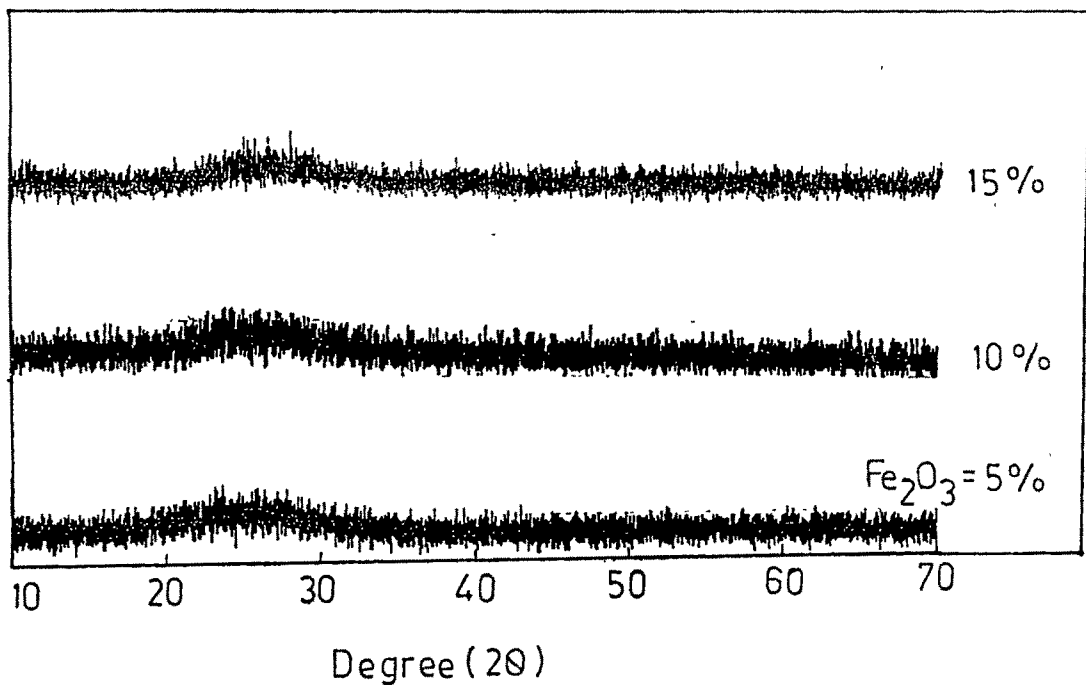
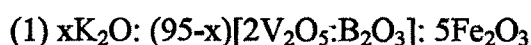


Figure 4.13 : X-ray diffraction pattern of few glass samples of Series 3.

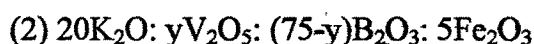
4.2 INFRARED SPECTROSCOPY:

4.21 INTRODUCTION:

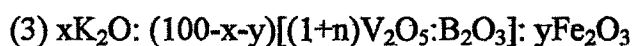
IR studies of the following series have been carried out to see the effect of glass modifier and glass former in the glasses. The change in molecular structure, bond lengths and vibrational groups have been studied with IR spectroscopy. Following four series have been prepared and studied.



Where $x=0$ to 30 in step of 5 mole %.



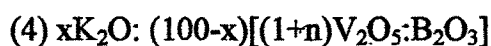
Where $y=40$ to 75 in step of 5 mole %.



Where $x=0$ to 20 in step of 5 mole %.

$y=5$ to 15 mole % in step of 2.5 mole %.

$n = 1$ to 2 in step of 0.2.



Where $x= 5$ to 20 in step of 5 mole % and $n=0.2$.

Figure 4.21 shows FTIR spectra of pure B_2O_3 , V_2O_5 and Fe_2O_3 , which are taken for the purpose of the comparison. It can be seen from the spectra [Figure 4.21 (a)] that B_2O_3 has characteristic absorption bands at 1471cm^{-1} , 1200cm^{-1} , 780cm^{-1} and 653cm^{-1} . The peaks at 1471cm^{-1} and 1200cm^{-1} are assigned to BO_3 triangle.^[1-3] The peak at 780cm^{-1} and 653cm^{-1} are attributed to bending vibrations of B-O-B bond^[2,4]. The B_2O_3 structure consists of BO_3 triangles, which are randomly oriented in three-dimensional network^[4-5] shown in Figure 4.22.

The Figure 4.21 (b) shows the FTIR spectra of pure V_2O_5 , which has characteristic features at 1020cm^{-1} , 850cm^{-1} and 613cm^{-1} . The V_2O_5 structure is built up by deformed VO_5 trigonal bonded in zigzag chains. Each VO_5 group

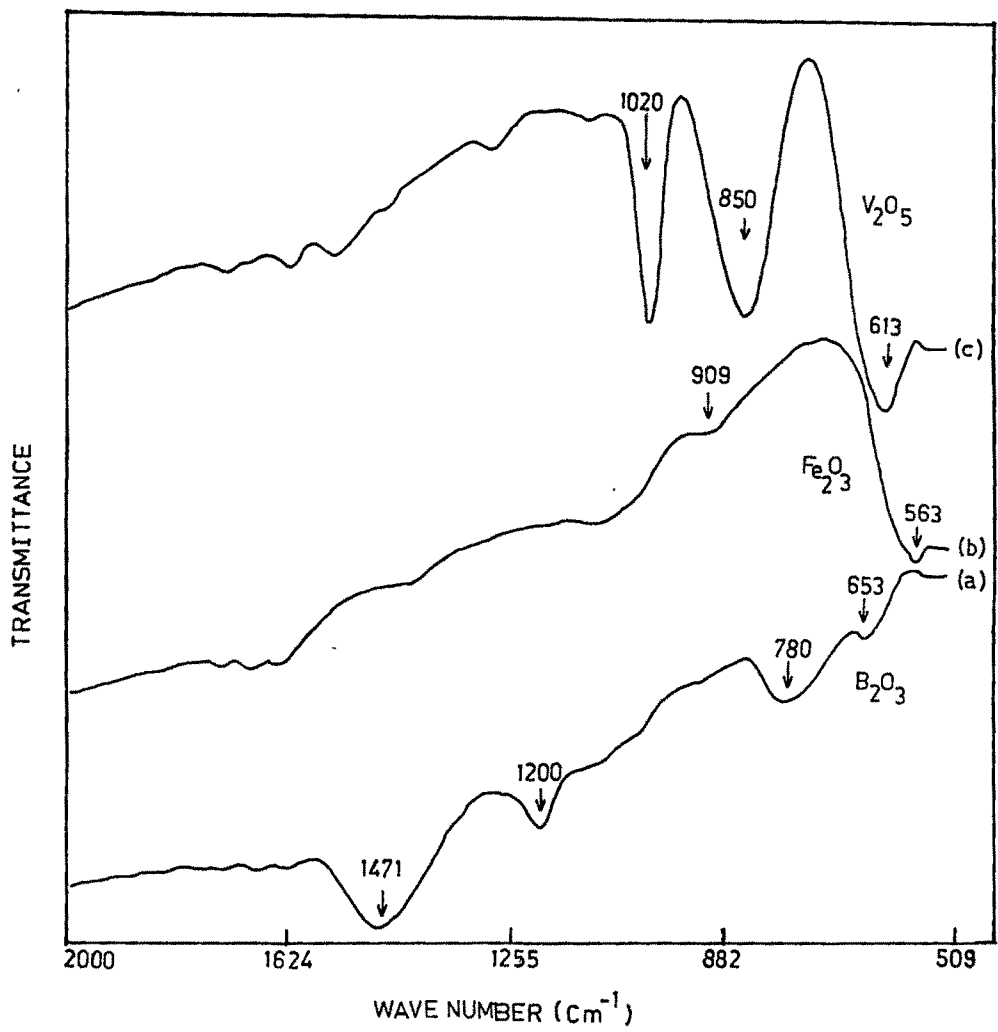


Figure 4.21 : FTIR spectra of pure V₂O₅, Fe₂O₃ and B₂O₃.

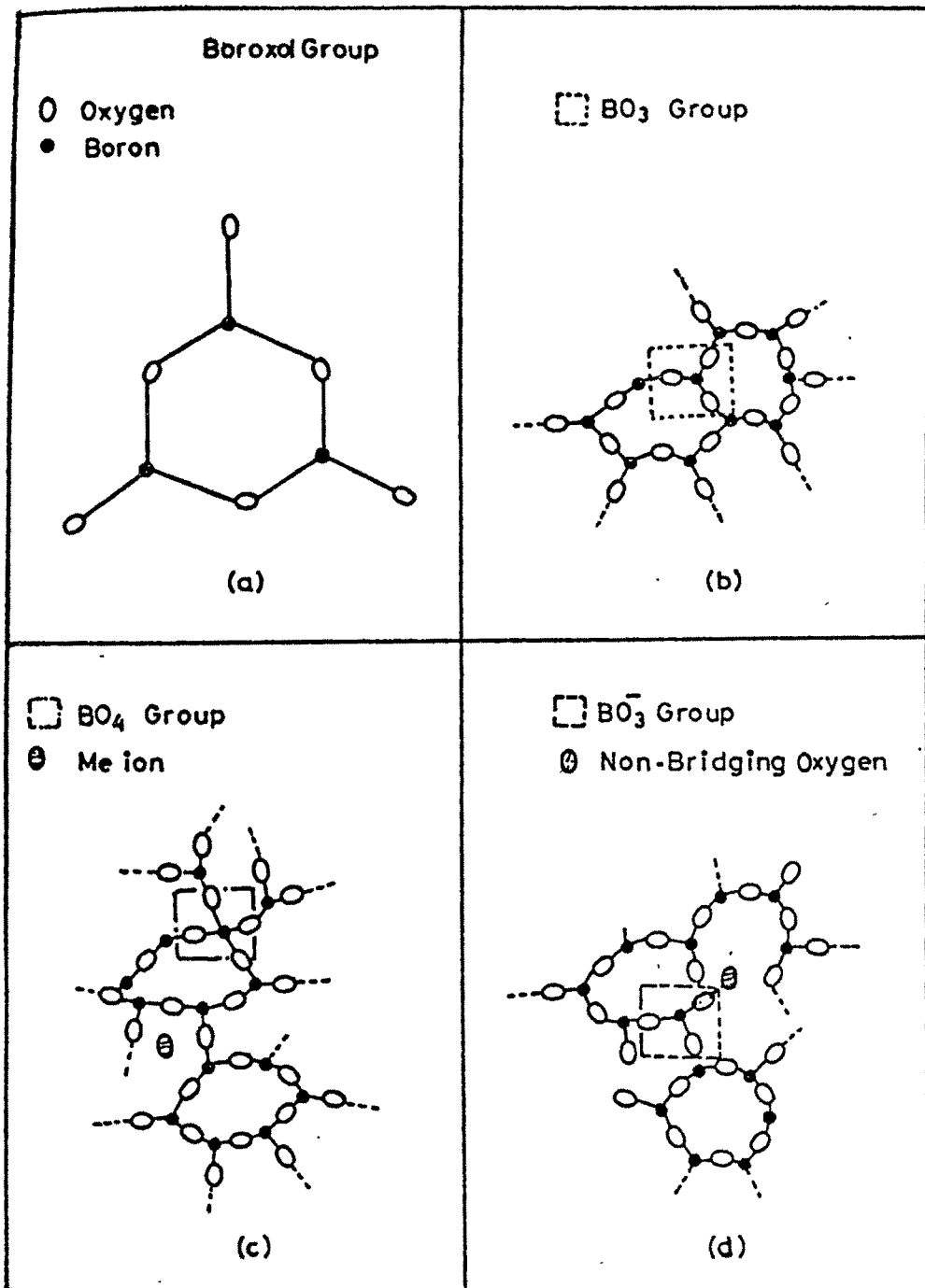


Figure 4.22 : Schematic diagram of various structural units.

contains a short V=O bond (vanadyl group)^[6]. The sharp band at 1020 cm⁻¹ is assigned to the vanadyl group of V=O bond whereas vibrations at 850 cm⁻¹ is related to symmetric stretching vibrations along V-O-V chain involved in corner sharing of VO₅ polyhedra^[7]. A very weak absorption peak present at 613 cm⁻¹ corresponds to V-O-V bond of symmetrical or bending mode of vibrations.

Figure 4.21 (c) for Fe₂O₃ have the characteristics feature at 563 cm⁻¹ attributed to the vibrations of FeO₄ groups of Fe₂O₃.

In the present study, the effect of glass modifier, network formers and Fe₂O₃ have been discussed.

4.22 EFFECT OF MODIFIER:

In the first series of the glass samples the amount of glass modifier K₂O is increasing whereas V₂O₅ and B₂O₃ are kept in ratio of 2:1 and the amount of Fe₂O₃ has been kept constant as 5 mole %. The FTIR spectra of all glass samples for K₂O = 0 to 30 mole % are given in Figure 4.23. The main features of IR spectra are being the appearance of resonance peaks at 1430 cm⁻¹, 1353 cm⁻¹, 1192 cm⁻¹-1253 cm⁻¹, 1104 cm⁻¹, 1000 cm⁻¹-940 cm⁻¹ and very weak and broad band between 804-602 cm⁻¹ and 860-651 cm⁻¹. Close examination of IR spectra reveals a very small shift of the vibrational band at 1430 cm⁻¹ up to 20 mole % of K₂O. When the amount of modifier, K₂O, is further increased, the vibrational band at 1430 cm⁻¹ splits into two vibrations 1353 cm⁻¹ and 1435 cm⁻¹, which are assigned to characteristics of B-O-B linkage in which both the borons are triangularly coordinated or -B-O< stretching vibrations^[8]. The peaks 1435 cm⁻¹ and 1353 cm⁻¹ slightly shift to 1437 cm⁻¹ and 1350 cm⁻¹ wavenumber at x=30 mole % of K₂O. In pure borate glasses the main structural element is the boroxol ring of plane trigonal configuration with B-O bond length 1.36 ± 0.005 Å, whereas, the B-O bondlength for BO₄ tetrahedra

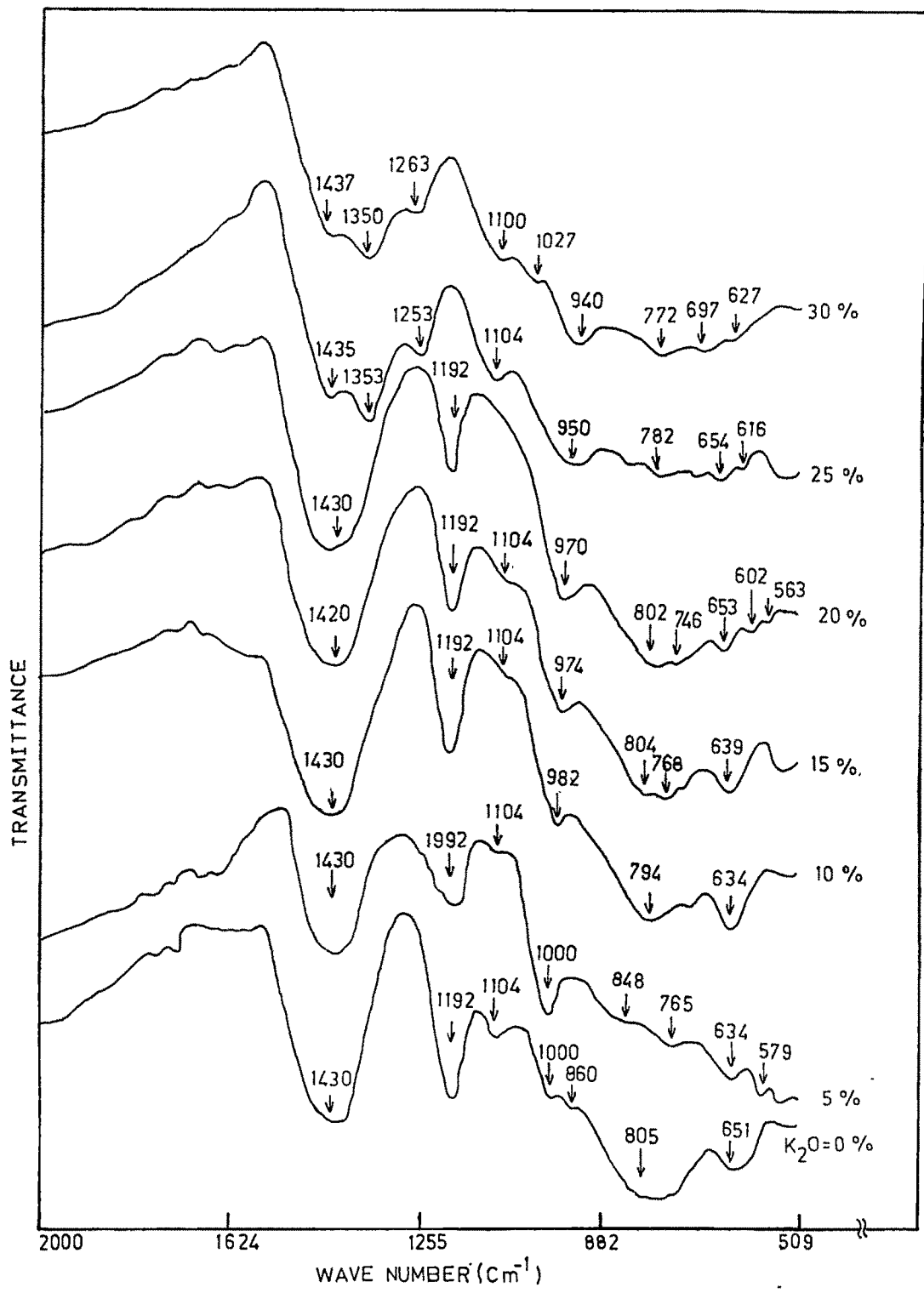


Figure 4.23 : FTIR spectra of $x\text{K}_2\text{O} : (95-x)[2\text{V}_2\text{O}_5 : \text{B}_2\text{O}_3] : 5\text{Fe}_2\text{O}_3$ glass series.

was observed to be $1.47 \pm 0.01 \text{ \AA}$. In IR spectra, the increase in bond length is seen as a shifting of an absorption band towards lower wavenumber. In binary borate glass, upto 14 %, K_2O does not break bridging in the BO_3 groups to form BO_4 tetrahedra. One K_2O causes the formation of two BO_4 tetrahedra, which participate in a three dimensional network, thus strengthening the structure^[9]. The B-O-B separation has been observed to increase which has been computed from density measurements^[4] (Section 4.4).

Another important feature of IR spectra is the presence of highly intense peak at 1192 cm^{-1} which is assigned to the boroxol group of BO_3 polyhedra (Figure 4.23). This peak remains present for $\text{K}_2\text{O}=0$ mole % to 20 mole % and above this, the peak disappears and a new vibrational band at 1253 cm^{-1} is observed, which is assigned to $=\text{B-O-B}=\equiv$ linkage in which one boron is tetrahedrally coordinated^[5]. Further, a disappearance of peak at 1192 cm^{-1} which is assigned to BO_3 linkage having boron in triangular coordination and appearance of peak at 1253 cm^{-1} in which boron has tetrahedral coordination may indicate that boron is now surrounded by more symmetric environment $=\text{B-O-B}=\equiv$ at tetrahedral coordination. For $\text{K}_2\text{O}=30$ mole %, a new weak absorption peak is observed at 1027 cm^{-1} which is assigned to the vibrations of BO_4 groups^[5] which also support the above mentioned fact of boron environment. For all glass samples from $\text{K}_2\text{O}= 0$ to 30 mole % a weak vibrational peak at 1104 cm^{-1} is observed which is assigned to the vibrations of non-bridging oxygens in the form of $=\text{B-O}^-$ or $\text{B-O}=\text{B}<\text{O}^{-[1,10-11]}$ indicating that the non-bridging oxygen are present even at $\text{K}_2\text{O}=0$ mole %.

Another distinguished feature of all glass samples are the vibrational band at 1000 cm^{-1} to 940 cm^{-1} which are assigned to isolated $\text{V}=\text{O}$ double bond of VO_5 polyhedra. With the addition of K_2O , the shift of this vibrational band towards lower wavenumber suggests the increase in bondlength of isolated $\text{V}=\text{O}$ bond. It is due to the fact that added K_2O goes into the structure at interstitial positions leaving its oxygens. K^+ ions now directly interact with the

oxygen of the V=O bond, which are thereby weakened and the frequency of vibration shifts towards the lower wavenumber. The added K₂O also gives rise to the formation of non-bridging oxygens, thereby creating VO⁻ unit [12]. It is obvious that the oxygen, which becomes non-bridging and acquires a negative charge will move closer to the connected vanadium, consequently reducing a positive charge on the vanadium ions and thereby resulting in a decrease in the binding of other oxygens attached to this particular ion; the length of the V=O bond therefore increases. Also, due to the irregular and random distribution of atoms in the glass structure, the K⁺ ions take position interstitial that are more symmetrical among other units. Therefore, V=O bonds are affected to different degrees depending upon the exact position that the potassium ion occupies. This fact is also supported by IR spectra of the heat treated glass samples^[2,12-13]. Therefore, the appearance of a broad absorption band and shifting towards lower wavenumber is thus expected. The presence of very weak and wide absorption band at 860 cm⁻¹ and 848 cm⁻¹-634 cm⁻¹ suggests that it is the sum of a number of absorption bands corresponding to V-O-V bonds of slightly varying bondlength and angles [12]. All the bands between 848 cm⁻¹-634 cm⁻¹ are significantly broadened which shift towards lower wavenumber sides because of short range order and such shifting in position of these peaks is attributed to changes produced in the structure of V₂O₅ due to the addition of glass modifier K₂O. As already mentioned, the absorption bands appearing at around 1000 cm⁻¹ to 940 cm⁻¹, 860 cm⁻¹ and 848 cm⁻¹ are due to vanadium phase and because of the glassy nature of the samples these bands are quite broad. Moreover, the glass forming ability increases with the increase of glass modifier K₂O^[2,14] and hence the broadening of the line. Therefore, it is difficult to pinpoint the exact position of any peak of these absorption bands except for that at 1000 cm⁻¹ to 940 cm⁻¹ which are attributed to V=O stretching vibrations.

The IR studies of $K_2O-V_2O_5$ ^[14], $Fe_2O_3-V_2O_5$ ^[15] and $Na_2O-V_2O_5-Fe_2O_3$ ^[13] glasses revealed the formation of non-bridging oxygens, breaking of the V-O-V chains, increase in the symmetry of V-O polyhedra, equalization of the lengths of V-O bonds and decrease in the coordination number of vanadium. The DSC studies (Section 4.3) of the present glasses showed that the glass transition temperature, T_g , decreases gradually from 251 °C to 196 °C as the amount of K_2O increases from 0 to 30 mole %. The decrease in T_g is generally ascribed to the decrease in coordination number hence, transformation of VO_5 polyhedra to VO_4 is thus expected. Generally, a vibrational band due to tetrahedrally coordinated boron is also expected near about 940 cm^{-1} . Hence, the peak near to 940 cm^{-1} may be due to the combined effect of borate and vanadium structure.

The presence of weak peak near around 650 cm^{-1} and 579 cm^{-1} may be attributed to the FeO_4 groups where its position remains unchanged. Hence, it is the modifier K_2O , which is responsible for bringing in the changes in vibrational bands related to borate and vanadate groups in the present glass series.

4.23 EFFECT OF GLASS FORMERS:

To observe the effect of glass formers, the IR spectra of the glasses of series 2 have been taken. The spectra of present glasses are very broad band and are entirely due to the vibrations of B_2O_3 and V_2O_5 species. Figure 4.24 shows the FTIR spectra of glass samples of series-2. IR spectra have characteristics features at 1400 cm^{-1} , 1264 cm^{-1} , 1088 cm^{-1} , shift from 950 cm^{-1} to 1020 cm^{-1} , 804 cm^{-1} and very weak absorption bands appeared at 740 cm^{-1} , 670 cm^{-1} and 617 cm^{-1} .

Two important bands at 1400 and 1264 cm^{-1} are assigned to B-O vibrations of BO_3 group and $=B-O-B\equiv$ linkage respectively ^[5]. The peaks at

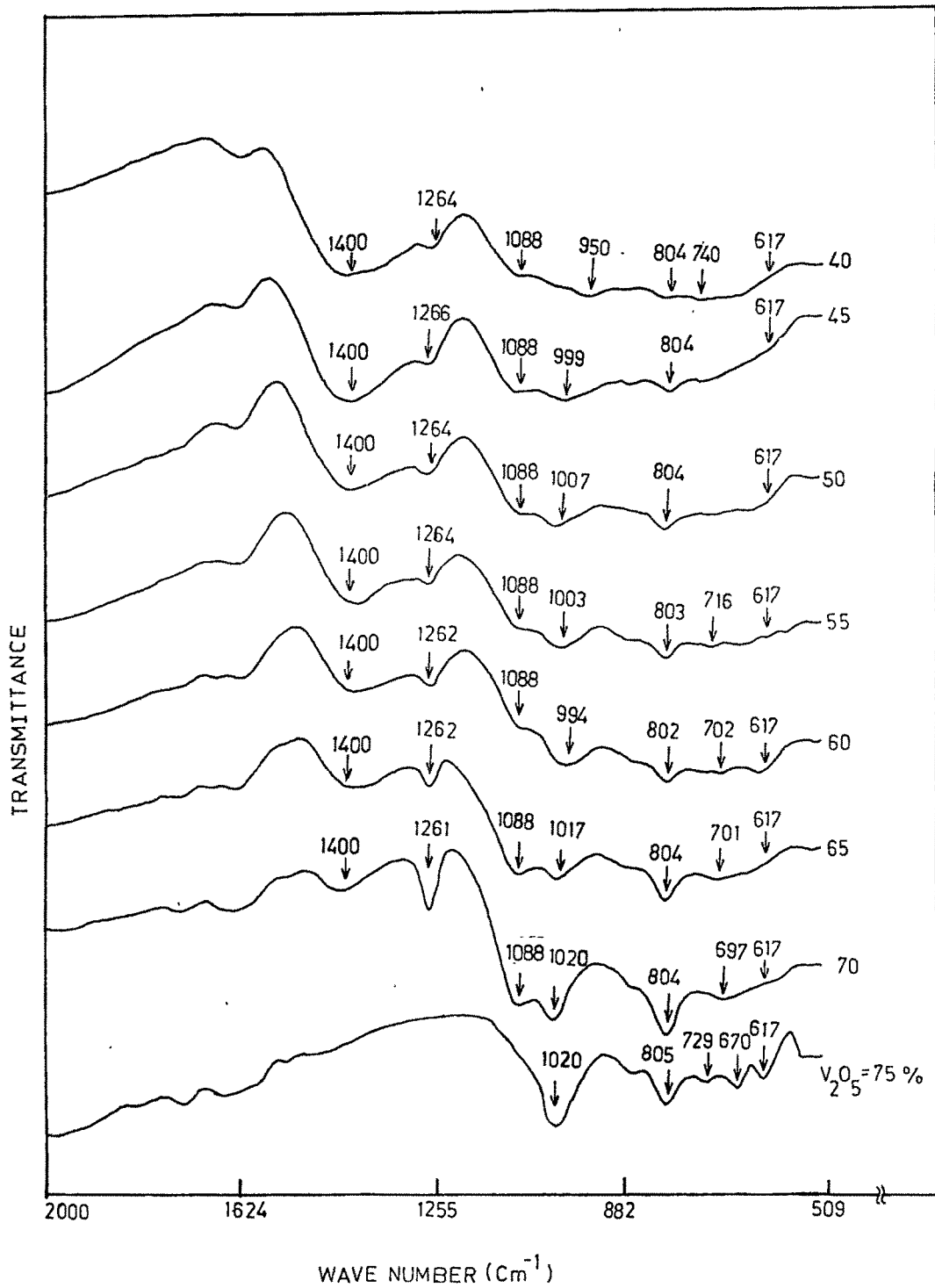


Figure 4.24 : FTIR spectra of $20\text{K}_2\text{O} : y\text{V}_2\text{O}_5 : (75-y)\text{B}_2\text{O}_3 : 5\text{Fe}_2\text{O}_3$ glass series.

1400 cm^{-1} , 1264 cm^{-1} , 1088 cm^{-1} and 804 cm^{-1} are due to the structure of B_2O_3 , which do not show any change in their positions which indicates that B_2O_3 structure is not affected much by gradual decrease of B_2O_3 amount in the glasses. With increase of y , a very small but noticeable decrease in intensity of 1400 cm^{-1} peak has been observed. Although with the increase of y , more amount of K_2O , which is fixed as 20 mole %, will be available for interaction with B_2O_3 and a lesser amount of K_2O with V_2O_5 , no major shift or change in B_2O_3 structure has been observed. It indicates that the available amount of K_2O for interaction with B_2O_3 is not sufficient to bring any noticeable changes in the IR spectra of B_2O_3 structure, whereas continuous increase of 940 cm^{-1} assigned to V=O bond to higher wavenumber with the increase of y supports the fact of continuous decrease in interaction of K_2O with V=O bond.

As the amount of V_2O_5 is increased from 40 mole % to 75 mole %, the vibrational band at 950 cm^{-1} which is assigned to V=O bond shifts towards a higher wavenumber 1020 cm^{-1} side with noticeable increase of the intensity. With the decrease of B_2O_3 , the glass forming ability of the glass composition also decreases. Hence at $y=75$ mole %, B_2O_3 amount in the glass is zero and a very sharp absorption peak at 1020 cm^{-1} is observed which is present in pure V_2O_5 glass matrix. Also, when no B_2O_3 is present in the glass for $y=75$ mole %, peaks at 1400 cm^{-1} , 1264 cm^{-1} and 1088 cm^{-1} are not observed in the IR spectra. The absence of the peaks at 1400 cm^{-1} for B-O vibrations of BO_3 group and 1264 cm^{-1} for =B-O-B≡ linkage is the clear indication of absence of B_2O_3 in the glass system at $y=75$ mole %. From $y=40$ to 70 mole %, a weak absorption peak at 1088 cm^{-1} , which is assigned to >B-O⁻ vibrations, shows the presence of non-bridging oxygens along with the formation of BO_4 groups^[1,10-11] in the glasses.

Another absorption band between 804 cm^{-1} -740 cm^{-1} is observed which is assigned to asymmetrical stretching vibrations of V-O-V chains^[4,16]. The position of these bands remains almost constant. The IR study of BaO- B_2O_3 -

V_2O_5 ^[4] and $K_2O-V_2O_5-B_2O_3-Fe_2O_3$ ^[2] also discussed the peak assigned to V-O-V group in which vibrations occurred at 820 cm^{-1} . At $y=75$ mole %, a number of sharp peaks are observed between 805 cm^{-1} – 617 cm^{-1} which are due to the absence of B_2O_3 which helps in increasing the glass forming ability and hence more amorphousness of the glass structure. IR Spectra have two more vibrations at 670 cm^{-1} and 617 cm^{-1} assigned to a weak vibrations of V-O-V chains involved in bending vibrations^[6] as well as to FeO_4 group of vibrations^[4,17]. Hence, these peaks are the resultant effect of FeO_4 and V-O-V bending mode, whose position remains unchanged in this series of glasses.

4.24 EFFECT OF Fe_2O_3

In this series, the effect of Fe_2O_3 in the glass samples has been carried out. Many authors^[3, 17-18] studied the effects of Fe_2O_3 on glass structure. Fe_2O_3 may play a role of network modifier or network former being amphoteric in nature^[3]. FTIR spectra of the present glasses in Figure 4.25 shows the characteristic feature at 1460 cm^{-1} , 1200 cm^{-1} , 1100 cm^{-1} , 1020 cm^{-1} , 920 cm^{-1} , 653 cm^{-1} , 797 cm^{-1} - 740 cm^{-1} and 605 cm^{-1} - 552 cm^{-1} . A very sharp intense band at 1460 cm^{-1} and 1200 cm^{-1} are assigned to a characteristic vibration of B-O bond of BO_3 groups. The absorption peak at 1460 cm^{-1} shifts towards a lower wavenumber with the increase of Fe_2O_3 amount resulting into the increase of B-O bond length and consequently converting to BO_4 units. The vibrational peak at 1200 cm^{-1} which is assigned to BO_3 group of vibrations disappears at $y=10$ mole % and a vibrational peak at 1260 cm^{-1} is observed, which is assigned to $=B-O-B\equiv$ linkage^[5].

A very weak absorption band at 1100 cm^{-1} which is assigned to the vibration of non-bridging oxygens in the form of $>B-O^-$ or $B-O=B<O^-$ ^[1,10-11] is present and whose intensity gradually decreases with the increase of Fe_2O_3 .

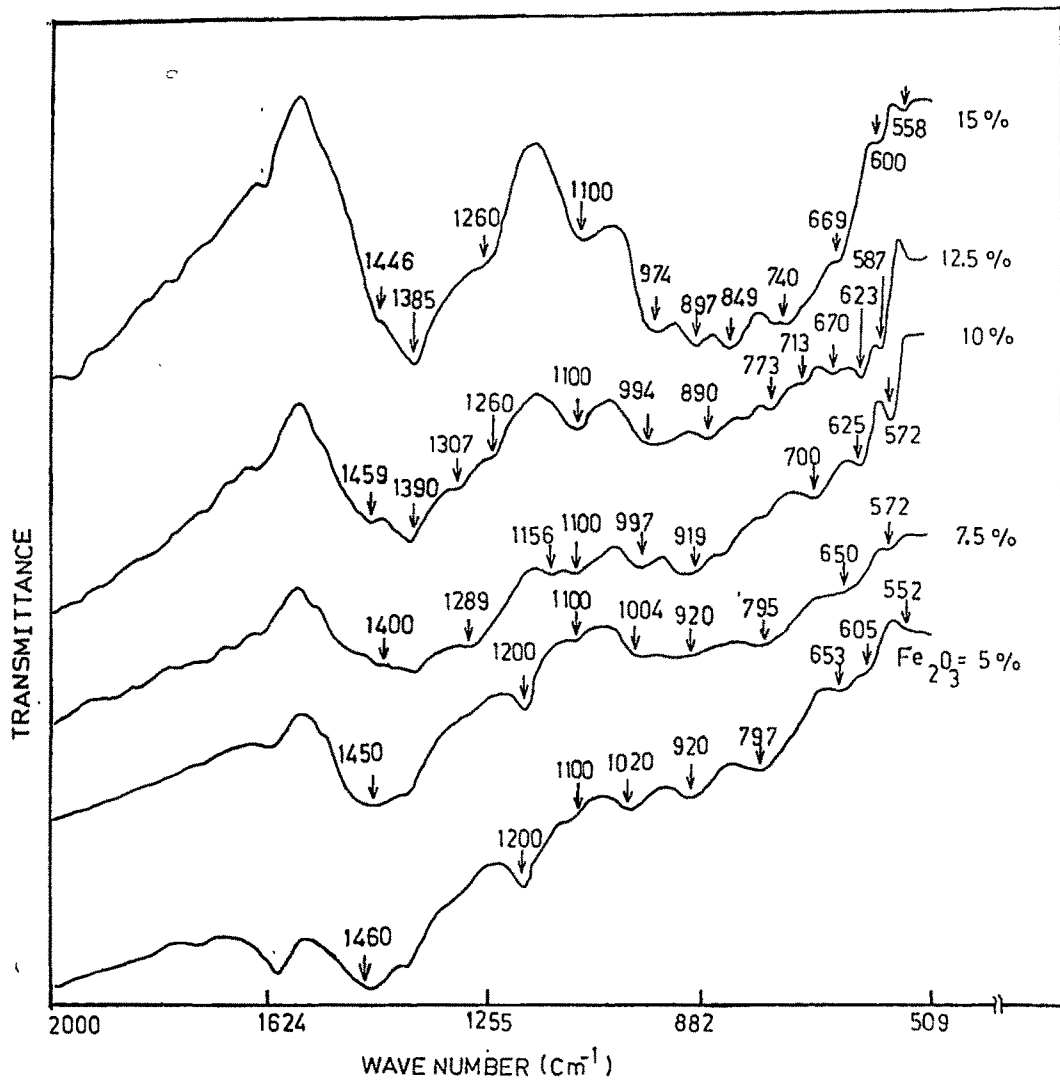


Figure 4.25 : FTIR spectra of $x\text{K}_2\text{O}:(100-x-y)[(1+n)\text{V}_2\text{O}_5:\text{B}_2\text{O}_3]:y\text{Fe}_2\text{O}_3$ glass series.

This peak remains present and does not shift for any of the glass samples for $\text{Fe}_2\text{O}_3=5$ to 15 mole %.

Fe_2O_3 may also cause the change in the structure of V_2O_5 . The peak at 1020 cm^{-1} is assigned to vibration of V=O bond in vanadyl group of VO_5 polyhedra, which shifts towards the lower wavenumber. The elongation of this bond due to K_2O is already discussed in the last Section 4.22. Fe^{+3} ions may also go at interstitial to bring change in V=O bond resulting into the shift of V=O bond peak from 1020 cm^{-1} to 974 cm^{-1} . To confirm the role of Fe_2O_3 in the glass structure, few glass samples in 4th series without Fe_2O_3 have been prepared and IR spectra are observed. Figure 4.26 shows the IR spectra of these glasses. The main characteristic features of the IR spectra are the presence of 1445 cm^{-1} , 1260 cm^{-1} , 1095 cm^{-1} , 1020 cm^{-1} - 990 cm^{-1} , 745 cm^{-1} - 785 cm^{-1} and 646 cm^{-1} - 669 cm^{-1} vibrational bands. The vibrational peak at 1445 cm^{-1} does not seem to shift neither to lower nor higher wavenumber side, whereas, the same peak in IR spectra of glasses of 3rd series, shifts towards the lower wavenumber side. However the peak at 1260 cm^{-1} and 1095 cm^{-1} remains unaffected but vibrational band of V=O bond at 1020 cm^{-1} shift to 990 cm^{-1} gradually and 745 cm^{-1} shifts to higher wavenumber i.e., 785 cm^{-1} . This clearly indicates that not only K_2O but also the presence of Fe_2O_3 certainly affects the structure of BO_3 and VO_5 units. Kishore et. al.,^[16] discussed that the addition of Fe_2O_3 accelerates the change in the boron coordination from BO_3 to BO_4 . The IR spectra of 3rd series have one more important feature at 920 cm^{-1} which remains absent in the first two series. Bansal et. al.^[4] discussed that the peak at 920 cm^{-1} assigned to V-O⁻ units and BO_4 units containing non-bridging oxygens, whereas, Dimitriev et. al.,^[15] discussed the same peak in conjunction with the symmetric and asymmetric vibrations of isolated VO_2 groups in VO_4 polyhedras. In the present glasses, the peak at 920 cm^{-1} can also be assigned to V-O⁻ and BO_4 units.

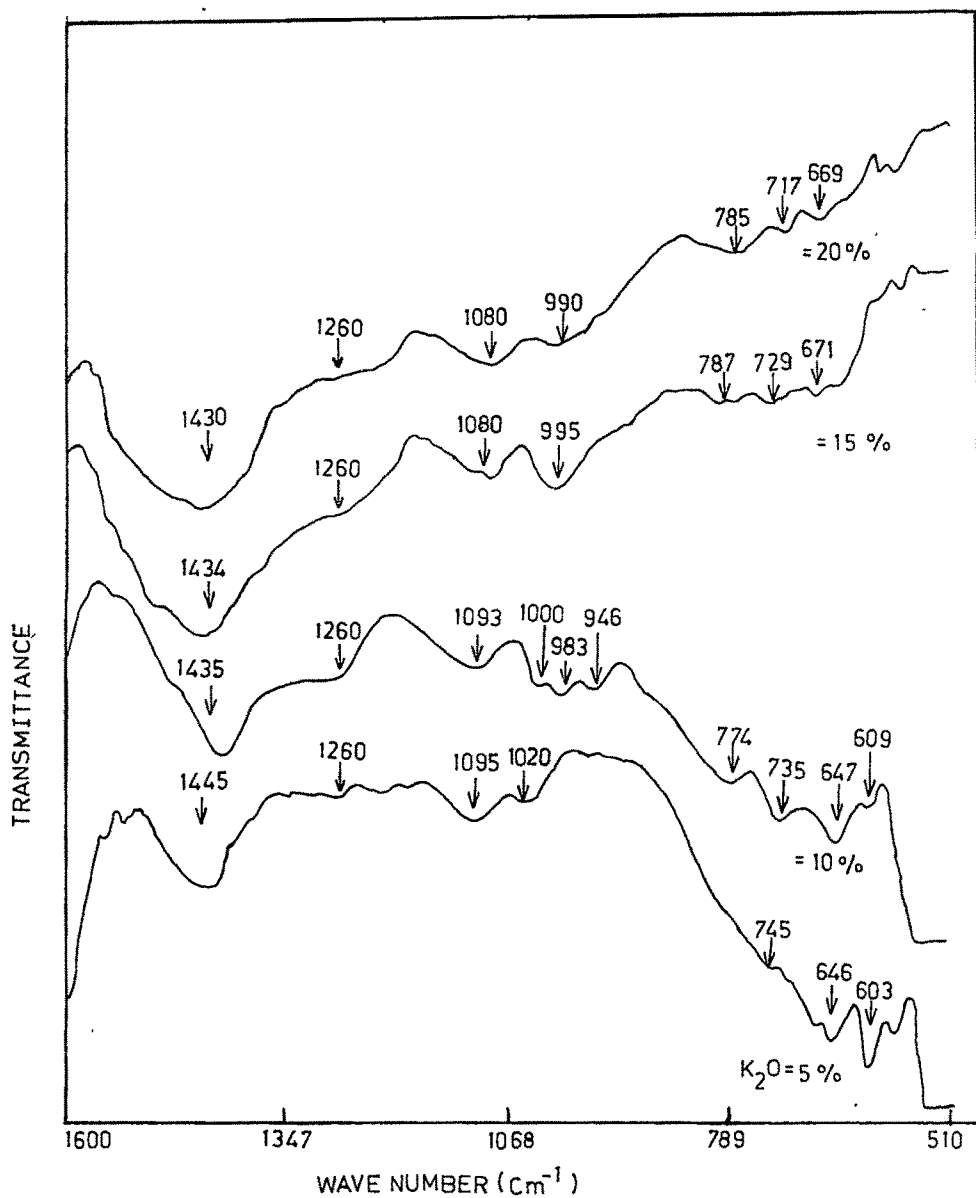


Figure 4.26 : FTIR spectra of $x\text{K}_2\text{O} : (100-x)[(1+n)\text{V}_2\text{O}_5 : \text{B}_2\text{O}_3]$ glass series.

The peak at 653 cm^{-1} and 605 cm^{-1} are assigned to the V-O-V bridging bonds of bending mode of weak vibrations in vanadate structure. The presence of very weak vibrations at 653 cm^{-1} and 552 cm^{-1} are possibly due to FeO_4 groups or non-spherical microcrystals of Fe_2O_3 present in the glass samples. Generally, the absorption peak at 653 cm^{-1} is assigned to V-O-V group of vibrations. Hence, these absorption positions may be assigned due to the resultant effect of both V-O-V and FeO_4 groups^[19-21].

Therefore, it can be ascribed that it is not only K_2O but Fe_2O_3 is also responsible in modifying the structure of BO_3 and VO_5 polyhedras in the glasses.

REFERENCES:

1. A. M, Sanad, I. Kashif, A. A. El-Sharkawy, A. A. El-saghir & H. Farouk, *J. of Mater. Sci.*, **21**(1986)3490.
2. D. K. Kanchan & H. R. Panchal, *Tr. J. of Physics*, Vol., **22**(1998)989.
3. I. Kashif, H. Farouk, A. M. Sanad, S. A. Aly & H. Farhan, *Phy. Chem. Of Glasses* Vol. **32**, No. 3(1991)87.
4. T. K. Bansal & R. G. Mendiratta, *Phys. & Chem. Of Glasses*, Vol. **28**, No. 6(1987)P.242.
5. Yoo Yong Kim, Keu Hong Kim & Jae Shi Choi, *J. Phy. Chem. Solid* Vol, 50, No.9 (1989) 903-908.
6. J. Krogh-Moe, *Phy. & Chem. of Glasses* Vol. **6**, No.2,(April 1965)P. 46.
7. H. G. Bachman, F. R. Ahmed & W. H. Barner, *Z. Kristallogh*, **115**(1961)110
8. L. D. Fredrickson & D. M. Hausen, *Analy. Chem.*, **35**(1963) 825.
9. Bratu P. Oana & Monica Culea, *Phy. Stat. Solidi (a)* **100**(1987)K195.
10. W. Vogel and N. Kriedle, *Chem. Of Glasses*, Pub. By Amm. Cerm. Soc. Ohio, Columbas, 1985.
11. S. Anderson, R. L. Bohem & D. D. Kimpton, *J. of Amm. Cerm. Soc.*, **38**(1955)370.
12. P. E. Jellyman & J. P. Proctor, *Trans. Soc. Glass. Technol*, **39**(1955)T173.
13. D. K. Kanchan, R. G. Mendiratta, R. K.Puri, *J. Mater. Sci.* **21**(1986)2418.
14. E. E. Khawaja, M. Sakhawat Hussain, M. A. Khan, J. S. Hwang, *J. Mater. Sci.* **21**(1986)2812.
15. Y. Dimitriev, V. Dimitriev, M. Arnaudov & D. Topalov, *J. Of Non. Cryst. Solids*, **57**(1983)147.

16. V. Dimitrov, Y. Dimitriev and V. Mihailova, *Monatshefte Fur Chemie* **114**(1983)669.
17. L. Rivolon, A. Revcolevschi, J. Livage & R. Collongues, *J. Non.-Cryst. Solids* **21**(1976)171.
18. N. Kishore, K. Aggarwal, R. Kamal & R. G. Mendiratta, *Phy. Chem. Of Glasses*, Vol. **23**, No. 6(1982)202.
19. Cheng Yibing, Y. U. Chao & Pan Shuying, *J. Of Non Cryst. Solids* **80**(1986)201.
20. N. Kishore, T. K. Bansal, R. Kamal, R. G. Mendiratta, *J. of Non-Cryst. Solids* **69**(1985)213.
21. R. Kamal, S. S. Shekhon, N. Kishore, R. G. Mendiratta, *J. of Non-Cryst. Solids* **53**(1982)227.

4.3 DIFFERENTIAL SCANNING CALORIMETRY:

The DSC thermogram of all glass samples were recorded at the heating rate of 20 °C/min. Figures 4.31 (a), (b) & (c) show DSC thermograms of few glass samples of series 1,2 and 3. In DSC thermogram, four types of transitions are possible.

- (i) Second order transition in which a change in the horizontal base line is detected.
- (ii) An endothermic curve peak caused by a fusion or melting transition.
- (iii) An endothermic curve peak due to a decomposition or dissociation transition and
- (iv) An exothermic curve caused by a crystalline phase change.

The number, shape and position of the various endothermic and exothermic peaks with reference to the temperature may be used as a means for the qualitative identification of the substance under investigation. Limb and Davis^[1] reported that for V_2O_5 - P_2O_5 - B_2O_3 glass system, there are two phase transition separation and subsequent crystallization of V_2O_5 is at 290 °C and 410 °C. Also, since the area under the peak is proportional to the heat-change involved, the technique is useful for the semiquantitative or in some cases, quantitative determination of the heat of reaction.

In the DSC thermogram, the endothermic shift in the baseline was observed at a certain temperature known as "glass transition temperature", T_g . An endothermic peak is observed at a high temperature is known as liquidus or "melting temperature" T_m . An exothermic peak was observed for all glass samples in series 1, 2 and 3 between T_g and T_m . This peak is due to crystallization of compounds^[2-3]. The corresponding temperature is known as "crystallization temperature", T_c .

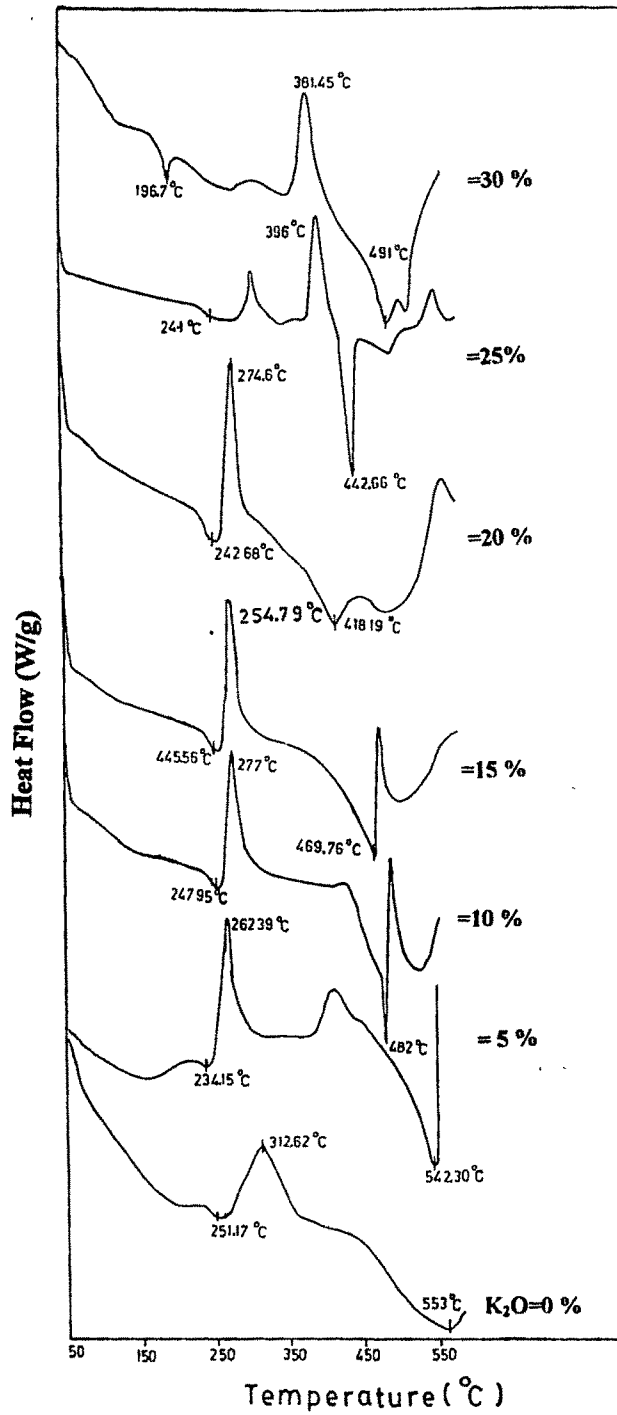


Figure 4. 31 (a) DSC thermogram of $xK_2O : (95-x)[2V_2O_5 : B_2O_3] : 5Fe_2O_3$ glass series.

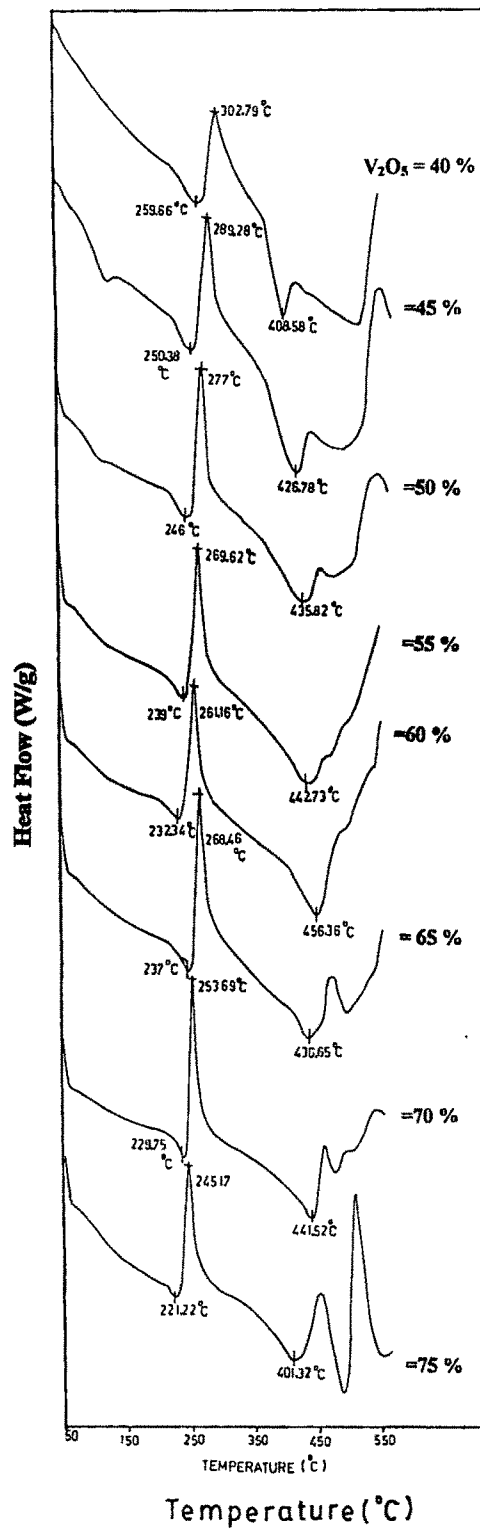


Figure 4. 31 (b) DSC thermogram of $20K_2O: yV_2O_5: (75-y)B_2O_3: 5Fe_2O_3$ glass series.

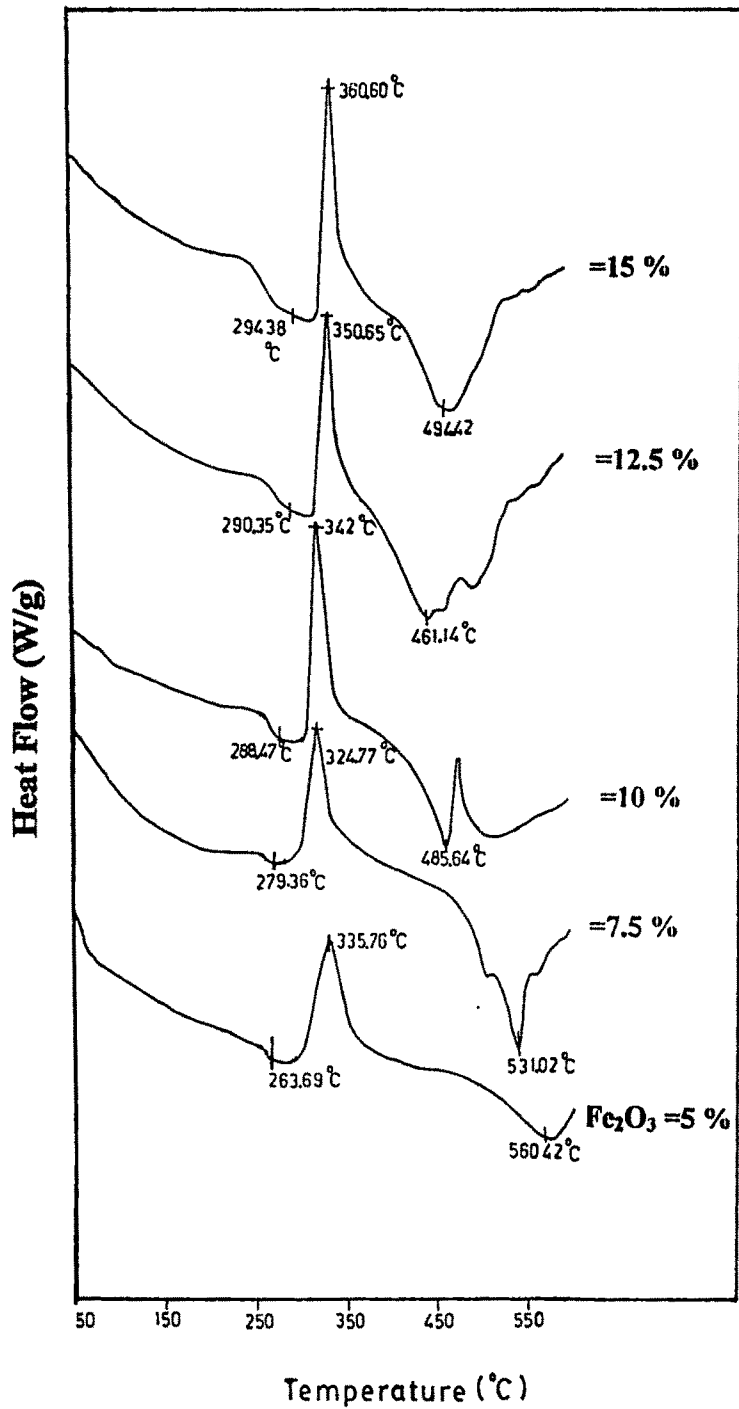


Figure 4.31(c) DSC thermogram of $x\text{K}_2\text{O} \cdot (100-x-y)[(1+n)\text{V}_2\text{O}_5 \cdot \text{B}_2\text{O}_3] \cdot y\text{Fe}_2\text{O}_3$ glass series.

The melting point depends upon the properties of both the liquid and crystalline phase, while the glass transition temperature, T_g depends only upon the characterization of the liquid phase. The ratio of T_g/T_m were calculated wherever it was possible to locate T_m . The observed values are shown in Table 4.31. The ratio lies about 2/3 for all glasses which is a characteristics of inorganic oxide glasses^[4]. DTA measurements were performed in order to establish the structural change of the glasses because the T_g is known to reflect the change in the coordination number of the network forming atoms and a destruction of the network structure brought about by the formation of non-bridging oxygens in the structure^[5-7].

The values of T_g are plotted against K_2O , V_2O_5 and Fe_2O_3 for series 1,2 and 3 respectively shown in Figure 4.32 (a), (b) and (c). It has been observed that the glass transition temperature T_g decreases with the increase of K_2O and V_2O_5 in series 1 and 2, whereas T_g increases with increase of Fe_2O_3 in series 3. The values of T_g , T_c and T_m are mentioned in Table 4.31 for all three series. A decrease in the T_g observed in the case of glass series 1 and 2 reflects a decreased coordination number of V^{+5} to V^{+4} and the formation of non-bridging oxygen atoms in the VO_4 tetrahedra. This is concerned with the decreased degree of bridging.

In case of glass series 3, T_g shows a distinct increase with the increase coordination number of the network forming atoms. This is concerned with the increased degree of bridging. The coordination number of boron atoms change from 3 to 4 which is also evident from the IR spectra of the present glass series^[8]. It has been reported that sodium tetraborate glass containing Fe_2O_3 showed an endothermic peak which shift to lower temperature as the Fe_2O_3 content is increased^[9]. Thus, with the help of DSC measurement it is possible to ascertain the structure and nature of glasses.

Table : 4.31 : DSC data of series 1, 2 and 3.

| $xK_2O: (95-x)[2V_2O_5:B_2O_3]: 5Fe_2O_3$ | | | | |
|--|-------------------------|-------------------------|-------------------------|-----------------------------|
| K_2O % | T_g | T_m | T_c | T_g/T_m |
| 0 | 251.17 | 553 | 312.62 | 0.45 |
| 5 | 234.15 | 542.3 | 262.39 | 0.43 |
| 10 | 247.95 | 482 | 277 | 0.51 |
| 15 | 245.56 | 469 | 275.79 | 0.52 |
| 20 | 242.68 | 418.19 | 274.6 | 0.58 |
| 25 | 241 | 442.66 | 396 | 0.54 |
| 30 | 196.7 | 491 | 381.45 | 0.4 |
| $20K_2O: yV_2O_5: (75-y)B_2O_3: 5Fe_2O_3$ | | | | |
| V_2O_5 % | | | | |
| 40 | 259.66 | 408.58 | 302.79 | 0.64 |
| 45 | 250.38 | 426.79 | 289.28 | 0.59 |
| 50 | 246 | 435.82 | 277 | 0.56 |
| 55 | 239 | 442.73 | 269.62 | 0.54 |
| 60 | 232.34 | 456.36 | 261.16 | 0.51 |
| 65 | 237.64 | 436.65 | 268.46 | 0.54 |
| 70 | 229.75 | 441.52 | 253.69 | 0.52 |
| 75 | 221.22 | 401.33 | 245.17 | 0.55 |
| $xK_2O: (100-x-y)[(1+n)V_2O_5:B_2O_3]: yFe_2O_3$ | | | | |
| Fe_2O_3 % | | | | |
| 5 | 263.39 | 560.76 | 335.76 | 0.47 |
| 7.5 | 279.35 | 531.02 | 324.77 | 0.53 |
| 10 | 288.47 | 485.64 | 342 | 0.59 |
| 12.5 | 290.35 | 461.14 | 350.65 | 0.63 |
| 15 | 294.38 | 494.42 | 360.6 | 0.6 |

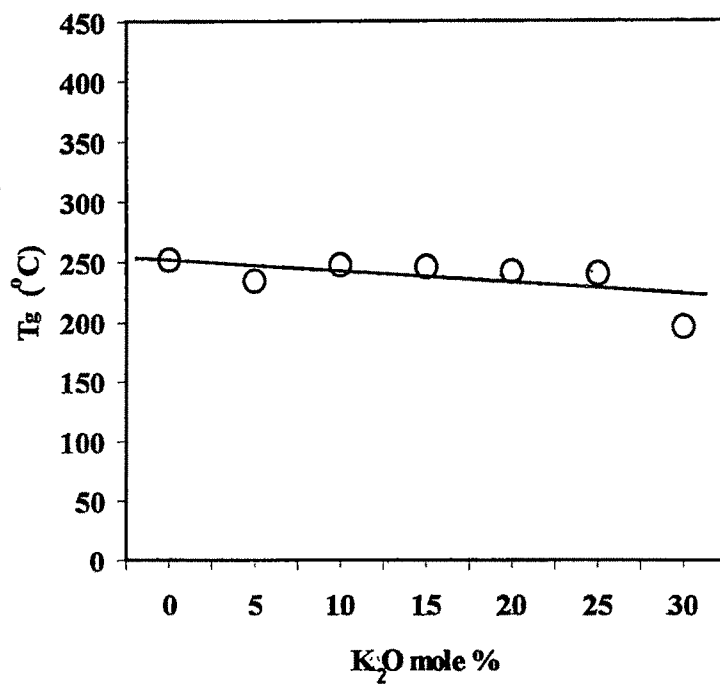


Figure 4.32 (a) Plot of glass transition temperature versus K_2O mole %

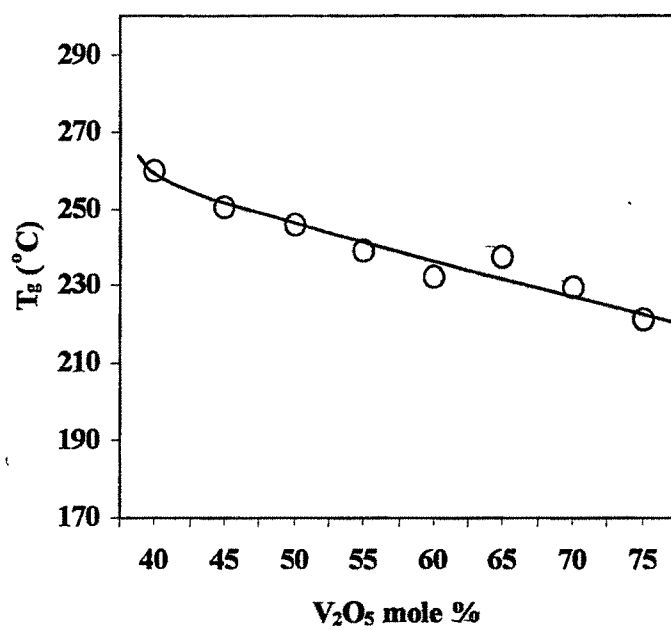


Figure 4.32 (b) Plot of glass transition temperature versus V_2O_5 mole %

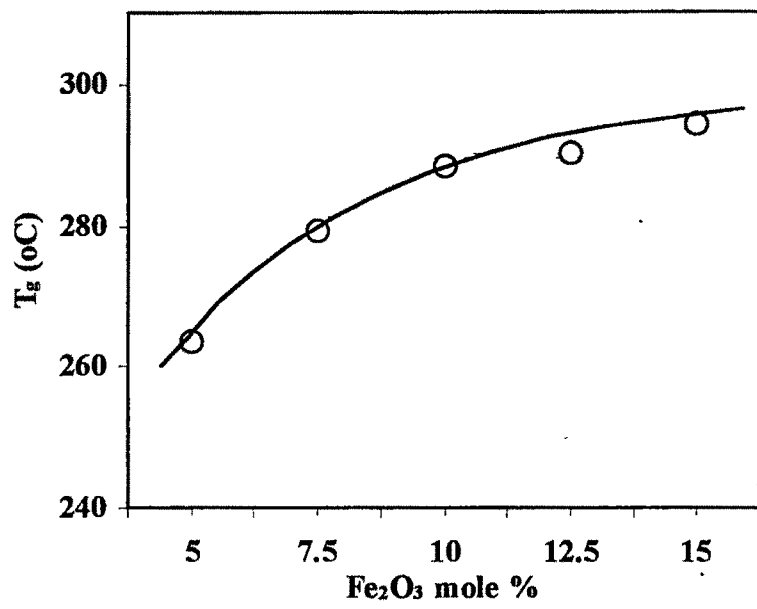


Figure 4.32 (c) Plot of glass transition temperature versus Fe_2O_3 mole %

Reference:

1. Y. Limb & R. F. Davis, Jr. of *Amm. Cerm. Soc.* **62**(1978)403.
2. T. I. Barry, D. Clinton, L. A. Lay, R. A. Merca & R. P. Miller, *J. of Mater. Sci.* **4**(1969)596.
3. D. Clinton, R. A. Mercer & R. P. Miller, Jr. of *Mater. Sci.* **5**(1970)171.
4. D. R. Uhlmann, A. G. Kelbeck & D. L. Dewitte, Jr. of *Non. Cryst. Solids* **5**(1971) 426.
5. T. Nishida & Y. Takashima, *Bull. Chem. Soc., Jpn.*, **60**(1987)941.
6. J. E. Shelby, *J. of Amm. Cerm. Soc.*, **57**(1974)436.
7. J. E. Shelby, *J. of Appl Phys.*, **46**(1975)193.
8. T. Nishida & Y. Takashima, *J. of Non-Cryst. Solids*, **94**(1987)22-237.
9. A. A. Kutub, *Jr. of Mater. Sci.* **23**(1988)2495.

4.4 DENSITY MEASUREMENTS:

The density of the glass samples were measured at room temperature by displacement method using methanol as the immersion liquid and single pan balance of 10^{-5} gm sensitivity. The measured values of density are given in the Table 4.41. It is observed from the Table 4.41 that a slight increase of density of glass samples are observed lying in the range of 2.65 gm/cc to 2.83 gm/cc and 2.64 gm/cc to 2.84 gm/cc for series 1 and 2 respectively. In case of series 3, the density of glass samples increases from 2.16 gm/cc to 2.98 gm/cc.

The density measurement were made to determine the number of transition metal ions per unit volume (i.e., Vanadium atoms), mobility of charge carriers and average spacing (V-V spacing) between these ions in the glasses. The number of transition metal ions were determined by assuming the glass structure as uniform i.e., all atoms are distributed uniformly which has helped in calculating the polaron radius^[1-2] by knowing the number of atomic sites per unit volume.

$$V_p = \frac{1}{2} \left(\frac{\pi}{6N} \right)^{1/3} \quad (4.41)$$

where, N is the number of sites per unit volume (i.e. V_{total} ions in V_2O_5). All the parameters calculated using density are shown in the Table 4.41. These parameters contributed towards an understanding of the electrical conduction mechanism, IR spectra, analysis of Mössbauer spectra, Seebeck coefficient, thermal and electrical switching mechanism in glass systems. Consequently, these measurement have helped in understanding the structure of semiconducting glasses.

Table 4.41 : Physical parameters calculated from density measurement for Series 1, 2 and 3.

| Series | Mole % | Density (gm/cc) | W (eV) | W_H (eV) | v_p (Å) | N (V_{total}) 10^{22} | B-B Spacing (Å) | V-V spacing (Å) | Fe-Fe spacing (Å) | σ_{100} $\Omega^{-1}Cm^{-1}$ | μ mobility $cm^2V^{-1}S^{-1}$ |
|----------|---------------|-----------------|--------|------------|-----------|-----------------------------|-----------------|-----------------|-------------------|-------------------------------------|-----------------------------------|
| Series 1 | $K_2O=0\%$ | 2.65 | 0.407 | 0.327 | 1.67 | 1.39 | 5.37 | 4.16 | 11.33 | 1.59×10^{-5} | 4.70×10^{-7} |
| | 5 | 2.71 | 0.411 | 0.332 | 1.68 | 1.37 | 5.54 | 4.18 | 11.18 | 3.55×10^{-6} | 7.50×10^{-8} |
| | 10 | 2.73 | 0.420 | 0.336 | 1.70 | 1.33 | 5.45 | 4.22 | 11.08 | 5.62×10^{-6} | 1.11×10^{-7} |
| | 15 | 2.75 | 0.442 | 0.339 | 1.72 | 1.28 | 5.52 | 4.27 | 11.00 | 1.59×10^{-6} | 3.10×10^{-8} |
| | 20 | 2.77 | 0.479 | 0.342 | 1.74 | 1.23 | 5.60 | 4.33 | 10.91 | 5.62×10^{-7} | 9.00×10^{-9} |
| | 25 | 2.83 | 0.509 | 0.347 | 1.76 | 1.20 | 5.65 | 4.37 | 10.76 | 4.47×10^{-7} | 7.00×10^{-9} |
| | 30 | 2.70 | 0.536 | 0.343 | 1.82 | 1.08 | 5.85 | 4.52 | 10.86 | 2.04×10^{-7} | 3.10×10^{-9} |
| Series 2 | $V_2O_5=40\%$ | 2.18 | 0.585 | 0.327 | 1.975 | 0.85 | 5.26 | 4.90 | 11.47 | 1.78×10^{-8} | 1.36×10^{-11} |
| | 45 | 2.50 | 0.572 | 0.337 | 1.843 | 1.04 | 5.37 | 4.57 | 11.13 | 2.51×10^{-8} | 1.99×10^{-10} |
| | 50 | 2.71 | 0.556 | 0.340 | 1.756 | 1.21 | 5.64 | 4.36 | 10.98 | 3.39×10^{-8} | 3.07×10^{-10} |
| | 55 | 2.75 | 0.522 | 0.336 | 1.716 | 1.30 | 6.12 | 4.26 | 11.07 | 1.29×10^{-7} | 1.50×10^{-9} |
| | 60 | 2.87 | 0.512 | 0.333 | 1.665 | 1.42 | 6.73 | 4.13 | 11.06 | 2.40×10^{-7} | 3.21×10^{-9} |
| | 65 | 2.90 | 0.501 | 0.327 | 1.635 | 1.50 | 7.77 | 4.06 | 11.16 | 4.47×10^{-7} | 7.84×10^{-9} |
| | 70 | 2.94 | 0.459 | 0.321 | 1.609 | 1.57 | 9.87 | 3.99 | 11.25 | 6.31×10^{-7} | 1.16×10^{-8} |
| Series 3 | 75 | 2.98 | 0.451 | 0.315 | 1.583 | 1.65 | - | 3.93 | 11.33 | 1.00×10^{-6} | 2.41×10^{-8} |
| | $Fe_2O_3=5\%$ | 2.64 | 0.410 | 0.343 | 1.738 | 1.25 | 4.70 | 4.31 | 10.99 | 2.40×10^{-6} | 5.82×10^{-8} |
| | 7.5 | 2.70 | 0.431 | 0.334 | 1.746 | 1.23 | 4.97 | 4.33 | 9.06 | 8.59×10^{-7} | 1.92×10^{-8} |
| | 10 | 2.76 | 0.455 | 0.327 | 1.760 | 1.20 | 5.24 | 4.37 | 8.69 | 5.13×10^{-7} | 1.06×10^{-8} |
| | 12.5 | 2.79 | 0.496 | 0.319 | 1.788 | 1.14 | 5.54 | 4.44 | 8.05 | 2.00×10^{-7} | 3.89×10^{-8} |
| | 15 | 2.84 | 0.506 | 0.313 | 1.820 | 1.08 | 5.84 | 4.52 | 7.52 | 7.94×10^{-8} | 1.46×10^{-9} |

Reference:

1. A. Ghosh and B. K. Chaudhari, *J. of Non-Cryst. Solids* **83**(1986)151.
2. C. H. Chung, D. Lezal & J. D. Mackenzie, *J. of Mater. Sci.* **16**(1981)422.